Title: Flood exposure analysis of road infrastructure – Comparison of different methods at national level

Authors: Tsolmongerel Papilloud[a,b,*],Veronika Röthlisberger[a,b], Simone Loreti[a,b], Margreth Keiler[a,b]

[a] University of Bern, Institute of Geography, Hallerstrasse 12, CH-3012 Bern, Switzerland
[b] University of Bern, Oeschger Centre for Climate Change Research, Mobiliar Lab for Natural Risks, Hochschulstrasse 4, CH-3012 Bern, Switzerland

∗***Corresponding author at:*** University of Bern, Institute of Geography, Hallerstrasse 12, CH-3012, Bern, Switzerland

Email addresses: tsolmongerel.papilloud@giub.unibe.ch (T. Papilloud),
veronika.roethlisberger@giub.unibe.ch (V. Röthlisberger),
simone.loreti@giub.unibe.ch (S. Loreti),
margreth.keiler@giub.unibe.ch (M. Keiler)

Declarations of interest: none

Acknowledgement: We thank the natural hazards group at the Swiss Mobiliar Insurance Company "die Mobiliar AG" for acquiring and compiling the communal flood hazard maps. We also thank the Federal Office for Spatial Development (ARE) for providing the major road network data.

FLOOD EXPOSURE ANALYSIS OF ROAD INFRASTRUCTURE – COMPARISON OF DIFFERENT METHODS AT NATIONAL LEVEL

Abstract

Assessing the flood exposure of infrastructure is crucial for sustainable flood risk management. We propose to define road exposure to floods as "any road segment/element located within a flood hazard zone". On the example of Switzerland, we develop and compare three methods to assess the flood exposure of the road infrastructure: absolute road area potentially flooded (method A), relative road area potentially flooded (method B), and a network-based approach using the edge betweenness centrality index (method C). The results are aggregated and ranked in grid cells of 2 km by 2 km for comparison. The ranks are directly proportional to exposure levels. The results present distinct spatial patterns; grid cells with higher values in method A indicate where more road surfaces are in a flood hazard zone (urban or high road density areas in flood plains), while method B highlights where most of the road surface is in flood hazard zones of predominantly mountainous areas of Switzerland. Higher values in method C present areas where the most-connected road links within a network are exposed to floods. Most of the grid cells that have higher values in method B than in method C indicate isolated mountain valleys that can be accessed only by a single road exposed to floods. The study demonstrates the importance of an appropriate choice of methods in flood exposure analysis. As exposure analysis is a key step in flood risk assessment, the presented results provide information essential for decision making in disaster risk reduction.

Keywords

flood exposure, road network, road area, edge betweenness centrality, spatial comparison, spatial network analysis

1. Introduction

Infrastructure is essential to the economic and social well-being of modern societies (Jenelius and Mattsson, 2015; Pant et al., 2017). It concerns a wide range of sectors from transportation to energy, water, education, health, information and communication technologies, and agriculture and food (Coppola and Coppola, 2015). Recently, infrastructure has undergone further development, with growing interdependence (Pregnolato et al., 2017) and an increasing dependence of people's daily business activities on infrastructure (Chiaradonna et al., 2008; Gheorghe et al., 2006; Graham, 2009). This phenomenon, combined with the higher frequency and intensity of flood events in recent decades (Kundzewiz et al., 2014; Messner et al., 2007; Munich Re, 2014), has led to rising losses and damage to infrastructure during flood events in Europe (Kundzewiz et al., 2014; Messner et al., 2007; Munich Re, 2014; Pregnolato et al., 2017). Furthermore, flood events, which are responsible for the failure of infrastructure elements, result in business shut-downs (Jongman et al., 2012a).

Avoiding significant economic losses requires the assessment of flood risk to infrastructure (Narayanan et al., 2016), in particular for the infrastructure that is critical for the functioning of our society and whose failure could lead to serious economic and social consequences and even to the loss of lives (Cabinet Office, 2010). Among the eleven critical infrastructures listed in the European Programme for Critical Infrastructure Protection (European Commission, 2005), our study will focus on transport infrastructure, which serves the whole economy of a country or a city by connecting the most central areas to the most remote regions.

The flood risk (R_{ah}) can be quantitatively expressed as a function of hazard, the exposed elements at risk, and their vulnerability in the hazard scenario (Birkmann and Welle, 2015; Fuchs et al., 2013):

$$R_{ah} = H_{ah} \times E_a \times V_{ah}, \tag{1}$$

where H_{ah} is the hazard type h covering area a, E is the exposure of assets in area a, and V_{ah} is the vulnerability of assets from area a to hazard type h. As shown in eq.(1), the knowledge of flood exposure is one of the components to quantify the flood risk to infrastructure and, consequently, to draw up proper plans for risk management (Balijepalli and Oppong, 2014; Jenelius and Mattsson, 2015).

Despite the simplicity of eq.(1), the quantity of exposure included there is not defined straightforwardly or uniquely. This is because the term is defined in several ways in the literature (Berdica, 2002; Jenelius and Mattsson, 2015; Jenelius et al., 2006; Seneviratne et al., 2012; UNISDR, 2016; Wang et al., 2011; Zio, 2016) and because of interchangeability between the concepts of exposure and vulnerability (Jenelius and Mattsson, 2015) often arising from the differences between researchers' research questions, aims, and disciplinary backgrounds (Berdica, 2002; Debionne et al., 2016). Also within studies of vulnerability and risk analysis to infrastructure, the terminology of exposure, vulnerability, and risk is used diversely (Wang et al., 2011; Zio, 2016). Jenelius and Mattsson (2015) state that the concept of exposure considers the impact for a single user under a particular disruption scenario. They also state that the exposure could be regarded as conditional vulnerability from a societal perspective. Among the several definitions of flood exposure (Jenelius and Mattsson, 2015; Seneviratne et al., 2012; UNISDR, 2016) we use that given by the United Nations Office for Disaster Risk Reduction (UNISDR, 2016, :18), which defines exposure as "a situation of people, infrastructure, housing, production capacities and other tangible human assets located in hazard-prone areas". We further propose to extend this definition of flood exposure to the road network as "any road segment/element located within a flood hazard zone".

Flood exposure is not only ambiguously defined, it is also analysed with different approaches and methods. One common method is spatial intersection or spatial overlay between flood hazard zones and assets. However, a detailed exposure analysis is only possible if explicit geographical data are available for assets and well-established flood hazard zones. This challenge is especially addressed for national exposure analysis by Narayanan et al. (2016). Jongman et al. (2012b) also address the issue that the results of global exposure analyses are strongly dependent on the methods applied. Several studies assess flood exposure of roads applying this classical spatial intersection of flood hazard information and different asset types at national scale (Hankin et al., 2016) and at regional scale (Hanslow et al., 2018; Kulp and Strauss, 2017; Ramirez et al., 2016).

Another class of methods derived from network science, has been employed to assess the exposure of roads networks, but not to floods. Network science focuses on the topology of networks (graphs): structures composed of nodes (also called vertices or intersection points), such as road junctions, and edges (links between two nodes), such as road segments (Costa et al., 2007). A network science approach allows to identify the most important road segments (edges) and junctions (nodes) within a road network to be identified by using "centrality measures", such as degree centrality, betweenness centrality, closeness centrality and eigenvector centrality. In particular, the edge betweenness centrality (EBC) (Girvan and Newman, 2002) identifies those road segments that act as bridge-like connectors between two parts of the road network; without these, the road network would be highly disconnected.

In summary, we conclude that different understandings of exposure and vulnerability of road infrastructure exist that are strongly dependent on the research focus, the aim of the specific study, and the disciplinary background of the researchers. Based on the different settings and ideas of these studies, their comparability is low, so researchers and practitioners are still challenged in choosing a study design appropriate to their needs.

The purpose of this study is threefold:
- to assess exposure of major road network to floods at Swiss national level;
- to compare the results of these methods in order to identify high exposure areas where risk managers may need to take preventive measures in priority; and
- to examine if any patterns on flood exposure exist throughout the study area.
To achieve this, the following steps are taken. We provide a brief overview of previous studies related to flood exposure methods and approaches in section 2 and highlight in more detail the existing challenges for flood exposure analysis for road networks. We describe the data used for this study in section 3. In section 4, we propose three different methods to quantify flood exposure of roads. To compare them, we apply a correlation analysis and a decile ranking for their results in 4 km^2 square cells.

All three methods allow to identify the Swiss regions where roads are highly exposed to floods (section 5.1). However, we are not only interested in the results produced by each method but in their differences or similarities too. In particular, we aim to know whether the first two methods we propose, that do not consider any network characteristics, produce different results from the network-based approach (section 5.2). In addition, we investigate potential boundary effects which could affect the network-based exposure calculation of the Swiss road network at national level. We perform this analysis by comparing the exposure calculation at national level to the one at regional level. Discussion (section 6) and concluding remarks (section 7) are followed.

2. Related work

It is essential to assess flood exposure as first step in analysing flood risk to any assets or systems. Analysis on exposure to floods is carried out with different approaches and methods.

2.1. Classical approaches for flood exposure assessment

The classical approaches for flood exposure assessment intersect areas of flood hazards and assets of interest and they are reviewed and categorised in Table 1. The scale

of the assessments reaches from global (e.g. Jongman et al. (2012b)) over national (e.g. Fuchs et al. (2015)) and regional (e.g. Hanslow et al. (2018)) to the district (e.g. Arrighi et al. (2019)) and municipal level (e.g. Figueiredo and Martina (2016)). Assets are mostly buildings, population and infrastructure facilities. Several studies consider roads: highways by Hankin et al. (2016) and Narayanan et al. (2016), different types of roads by Hanslow et al. (2018); Kulp and Strauss (2017); Ramirez et al. (2016). These exposure analysis for roads mostly measure total length of road elements in flood hazard zones.

According to the description of exposure, spatial intersection operation is often applied between assets and hazard zones. For example, spatial intersection is used by (Figueiredo and Martina, 2016; Fuchs et al., 2015; Röthlisberger et al., 2017) to assess buildings' exposure to natural hazards; by (Hankin et al., 2016; Narayanan et al., 2016; Pant et al., 2017; Qiang, 2019) for infrastructure; and by Kappes et al. (2012) for both buildings and infrastructure. Flood hazard zones are of many different sources such as torrential flooding, river flooding and coastal flooding (Fuchs et al., 2015; Hankin et al., 2016). According to Table 1, quantification of exposure is expressed as such number of buildings, length of roads, or number of population, i.e. quantity of exposed assets. A common approach in this context of exposure analysis is to normalise the exposed assets per area (m^2, km^2, etc.) for allowing a better comparability of different spatial pattern. In contrast to this, Röthlisberger et al. (2017) consider two types of measures for exposure: absolute amount of exposed assets and ratio of exposed assets to total amount of assets in a certain area.

Table 1: Categorisation of methods on flood exposure analysis, ordered by scale.

Reference	**Purpose**	**Scale**	**Assets**	**Hazards**	**Methods**
Jongman et al. (2012b)	Global exposure to river and coastal flooding	Global	Population, land use and socio-economic data	River and coastal flood extent areas	Extract by flood hazard areas (i.e. **spatial intersection**); Quantification by exposed assets, which is derived from exposed people
Hirabayashi et al. (2013)	Global flood risk under climate change	Global	Global gridded population dataset	Simulated inundation area	**Simple overlay**; Quantification by number of people per grid, then summed for the total number of people
Fuchs et al. (2015)	Assessment of exposure analysis	National	Buildings, primary residents (registered to the buildings)	Torrential flooding, river flooding, snow avalanches	**Spatial intersection**; Quantification by number of buildings for each property type
Hankin et al. (2016)	Flood risks from multiple sources	National	National Strategic Road Network	River flooding and coastal flooding, flood map for surface water areas susceptible to groundwater flooding	**Spatial overlay**; Quantification by road length in 1 km grid cell
Hu et al. (2016)	Spatial exposure of infrastructure systems	National	Energy, transport and waste with their users	Flooding and drought hazards	**Spatial overlay**; Hotspot analysis using Kernel density estimation;
Narayanan et al. (2016)	Characterising national exposures to infrastructure from natural disasters	National	Infrastructures	FEMA SFHA for riverine flooding	"Simple geospatial comparison" (i.e. **simple overlay**); Quantification by number of facilities

Röthlisberger et al. (2017)	Exposure analysis, identifying hot spots	National	Buildings, residents (registered to the buildings)	River flooding	**Spatial intersection**; Quantification in two different units (municipality and a grid cell of similar size as municipality) by two types of exposure indicators: the **density** of exposed assets and the ratios of exposed assets. Hot spot analysis (Getis-Ord Gi*)
Qiang (2019)	Flood exposure of critical infrastructures in the US	National	Critical Infrastructures (CI)	FEMA flood maps	**Overlay**; Quantification by number and ratio of CI elements at national and state level; Statistical analysis: 1) Getis-Ord Gi* statistic for clusters and 2) Ratio of the infrastructure flood exposure is compared with the baseline ratio
Pant et al. (2017)	Critical infrastructure impact assessment (vulnerability analysis)	Catchment area (Thames)	Critical infrastructure (electricity, airports, ports, water, and waste water, telecommunications)	Flood likelihood map	**Spatial intersection**; direct exposure of network assets to flood hazard.
Kappes et al. (2012)	Multihazard exposure analysis tool	Regional level (Basin)	Building, infrastructure, settled area	Five natural hazards: debris flows, rock falls, shallow landslides, avalanches, and river flood	**Spatial overlay**; Quantification by number of building

Hanslow et al. (2018)	Current and potential future exposure analysis	Regional	Transport infrastructure	Estuary inundation due to sea level rise	**Spatial overlay**; Quantification by length of road including road type
Ramirez et al. (2016)	Test the performance of dynamic reduced-complexity model, Flood impact assessment	Regional (3 different sites)	Population, road and agriculture	Storm tide flooding	**Spatial overlay**; Quantification by total population, road length and agricultural area
Arrighi et al. (2019)	Mobility disruption by floods	District	Population, drivers and cars	Flood maps	**Overlay**; Quantification by number of people, drivers or cars
Figueiredo and Martina (2016)	Development of exposure data sets	Municipality	Buildings, population	Flood hazard map	**Spatial overlay**; Quantification by building footprints categorised by number of storeys
Kulp and Strauss (2017)	Coastal flood exposure	Municipalities in US coastal area	Population, housing unit, road length and property value	Inundation due to sea level rise	**Overlay**; Quantification by road length and expected annual exposure growth rates.

2.2. Network approach in flood exposure analysis

Analysis of flood exposure of road system could possibly be approached by the network perspective, which focuses on the topology and structure of the network. Several centrality measures are used to assess importance or connectedness of edges or nodes in the road network like degree centrality, betweenness centrality or and closeness centrality. For example, Demšar et al. (2008) incorporated edge betweenness centrality in vulnerability risk analysis for the Helsinki metropolitan area transport network. They claim that links with high value of betweenness are the most important elements in the network and consequently that vulnerability studies should focus on them. However, they did not consider any hazard condition. Similarly as for a city level, Casali and Heinimann (2019) applied betweenness centrality and closeness centrality for Zurich city road network. This study considered flood scenarios and aimed to determine changes in topological properties of the city network due to floods. Another example of applying centrality measure to urban road network is, the ranking-betweenness centrality, which is for evaluating network by its nodes ranks (Agryzkov et al., 2014). All the mentioned studies used traditional methods of network science such as centrality measures to identify critical elements of the network. However, there is a lack of analysing the general applicability of these methods for transport network beyond urban/city scale in the context of exposure.

Another alternative approach for identifying critical links in the network was suggested by Helderop and Grubesic (2019) by extending the edge betweenness centrality measure and taking into account the road segments' continuity in the landscape, which are non-network features. This method was applied for a small network in highly urban coastal area. Jenelius et al. (2006) studied the vulnerability of the road network of northern Sweden by applying link importance indices and site exposure indices. Conceptually, they considered that exposure is one part of the vulnerability and it accounts the consequences. Balijepalli and Oppong (2014) included the importance of the road link to the functioning of the network in a dense urban area of York to develop a range of indices for road network vulnerability to different flood scenarios. Kermanshah et al. (2017) included edge betweenness centrality as one of the variable in vulnerability assessments of road systems to floods in several cities in the USA.

In summary, this study addresses the following gaps in current knowledge and practice:
- There is no single criterion or method for measuring the flood exposure of a road segment; which approach is optimal seems to depend on the question to be answered in different areas of risk management.
- A comprehensive study that considers flood exposure, including hazard information and the road infrastructure at national level, is still lacking.
- Exposure is usually included in the vulnerability analysis without separating the analyses of exposure and vulnerability.
- Despite extensive literature searches, we could not find any study that compared different methods of assessing road network exposure to floods at national scale.

To fill the gaps, we propose three methods to quantify flood exposure of roads at national level. The first method calculates the road area that is potentially flooded, and the second method considers the relative amount of exposure as the ratio of the road area that is potentially flooded. However, for assets such as road networks, where links are crucial to functionality, additional criteria could be useful for assessing their

exposure. Therefore, we propose a third method that employs an edge betweenness centrality to identify the most connecting road segments within flooded areas.

3. Data

In this study, the data used to develop and compare the three methods are: (i) data on roads and traffic (see 3.1), (ii) data on flood hazard zones (see 3.2) and (iii) the swissBOUNDARIES3D dataset (Federal Office of Topography, 2017).

Geographic data on administrative boundaries and biogeographic regions from Federal Office of Topography (2017), and Aquaprotect from Federal Office for the Environment (2008) are publicly accessible. Major road network data is provided by Federal Office for Spatial Development ARE (2016) under contract and is currently not accessible to public. For the analysis of a complex network, the graph representation of the major road network in this study consists of 13421 vertices and 17658 edges. Cantonal flood hazard maps are aggregated for national level and provided by Mobiliar Lab (2017). It is renewed every half-year and also not accessible to the public. Summary of the input data sets is presented in Table 2.

Table 2: Summary of the data sets *(links are last checked on 25 February, 2020)*

Data	**Name**	**Description**	**Source**	**Open access**
Flood hazard zone maps	Flood hazard maps	Official Swiss cantonal fluvial flood hazard maps compiled in a single data set and provided by Swiss Mobiliar	`https://www.bafu.admin.ch/bafu/en/home/topics/natural-hazards/state/maps.html`	No
Flood hazard zones	Aquaprotect	Swiss-wide overview of the potential flood hazards with a 250-yr return period provided by the Swiss Federal Office for the Environment (2008; FOEN) based on a statistical modelling approach	`https://www.bafu.admin.ch/bafu/fr/home/themes/dangers-naturels/info-specialistes/situation-de-danger-et-utilisation-du-territoire/donnees-de-base-sur-les-dangers/aquaprotect.html`	Yes
Major road network	Swiss transport model	Swiss national and state roads with number of lanes, road segment length, speed limit, and daily traffic information by count of vehicle types and provided by the Federal Office for Spatial Development (ARE)	`https://www.are.admin.ch/are/en/home/transport-and-infrastructure/data/transport-perspectives.html`	No
Administrative boundary	swissBOUNDARIES3D	All administrative units of Switzerland and national boundaries and provided by the Swisstopo	`https://shop.swisstopo.admin.ch/en/products/landscape/boundaries3D`	Yes

Biogeographic regions	Biogeographical regions	The biogeographical regions of Switzerland are based on a purely statistical classification approach based on the mapping of Swiss flora by the CRSF and faunistic data by the CSCF.	https://opendata.swiss/de/dataset/biogeographische-regionen-der-schweiz-ch	Yes

3.1. Road and traffic data

The major road network data, which includes the Swiss national and state roads only, was employed in this work as road data. This dataset was provided by the Federal Office for Spatial Development (ARE) and was chosen for the availability of information about road segments, such as number of lanes, road segment length, speed limit, and daily traffic information by count of vehicle types. In addition, this dataset is currently used as basic information for the Swiss transport models (ARE, 2016). The number of lanes, the road segments lengths and the speed limits contained in the ARE dataset, were used to estimate two fundamental quantities for assessing the flood exposure with our proposed methods, i.e. the road surface and the travel time per each road segment, respectively. In particular, the road surface of each segment was estimated as the area of polygons created around the road segments, with the same road segment length and average road width equal to the number of lanes, times an average lane width of 3.5 m. This average width for a lane is estimated, since the major roads were originally represented as lines in the geographic information system (GIS). In GIS, polygons were created by a buffering operation. The speed limits, instead, were used to derive the travel time for each road segment. From a vehicle driver's or passenger's perspective, we assume that the travel time is the most important factor for trips between origin and destination; in other words, the shorter the travel time, the more important the road segment is (Pregnolato et al., 2017; Scott et al., 2006). The major road network is shown in Figure 1 and it is modelled such that a road junction is a node (or vertex), and a road segment is a link (or edge) in a graph representation.

3.2. Flood hazard zones

We use a compilation of flood hazard zone maps based on two sources: (i) communal flood hazard map and (ii) a nationwide floodplain model called Aquaprotect (Röthlisberger et al., 2017). In Switzerland, each canton compiles communal hazard zone maps that are created at the local municipal or cantonal level based on the federal hazard zone directive (Borter, 1999; Loat and Petrascheck, 1997) and according to its own requirements (Kunz and Hurni, 2008). We consider the low, medium, and high hazard zones of communal flood hazard maps (version by November 2017), which represent events with a return period of up to 300 years. Since the communal hazard maps are mostly focused on settlements, they do not cover the entire study area. Therefore, we complement them with the Aquaprotect flood hazard zone map. Aquaprotect data is a Swiss-wide overview of the potential flood hazards with a 250-yr return period provided by the Swiss Federal Office for the Environment (2008; FOEN) based on a

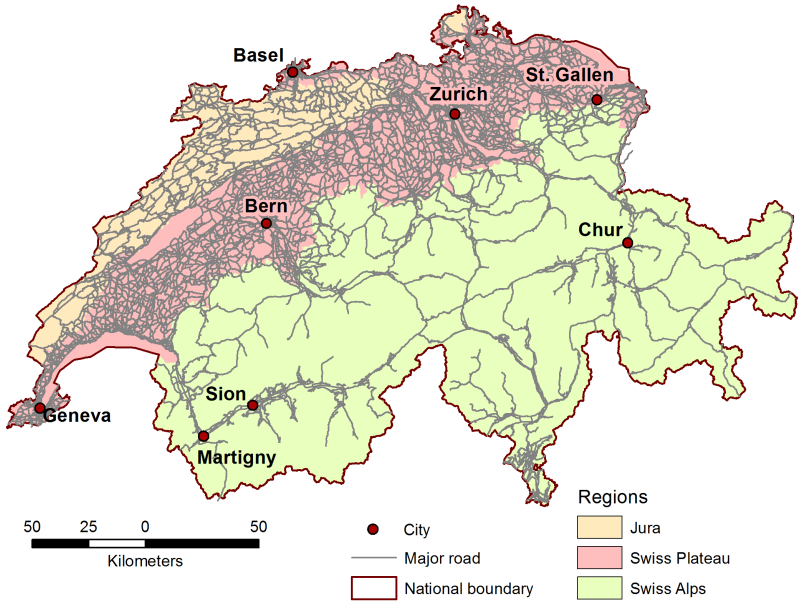

FIGURE 1. Swiss major road network and biogeographic regions.

statistical modelling approach (Federal Office for the Environment, 2008). This way, we generate a nationwide comprehensive and comparable map of flood hazard zones with return periods of 250 and 300 years. The major roads situated in flood hazard zones are shown in Figure 2. They are the result of spatial intersection between major roads and flood hazard zones. Also, the cantons of Zurich, Grisons, and Ticino are indicated in Figure 2.

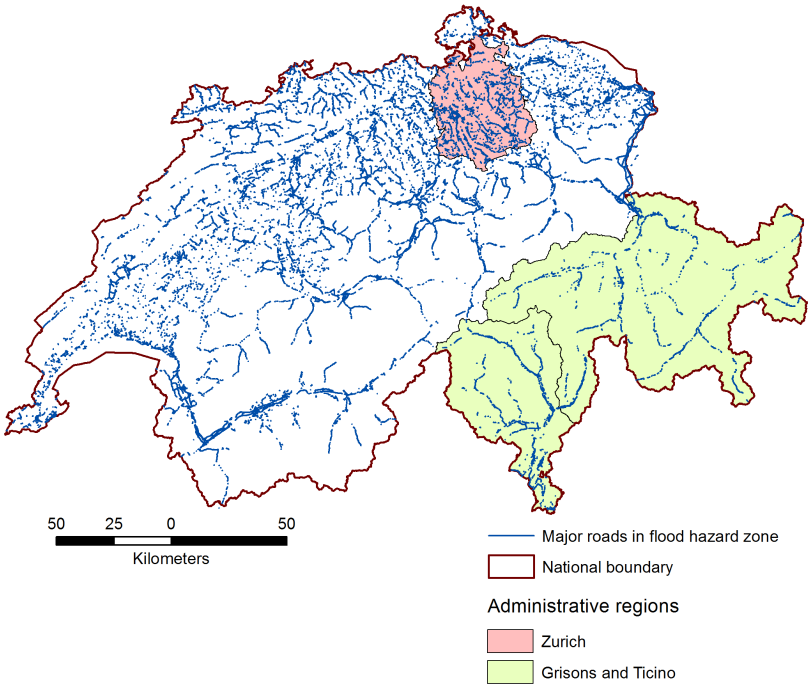

FIGURE 2. Major road segments intersected with the flood hazard zones

4. Methods

For assessing flood exposure of roads at national level, the first step is to overlay the road polygons with the flood hazard zones, which results in potentially flood-exposed road polygons. Then, a grid of 2 km by 2 km (4 km^2) square cells is generated and laid on top of the study area, intersecting the polygons of potentially flood-exposed road segments. Grid allows researchers to summarise characteristic values of geographic elements within a grid cell such as lengths (Hankin et al., 2016) or areas (Figueiredo and Martina, 2016).

Different grid sizes such as 4 km by 4 km, 1km by 1km and 0.5 km by 0.5 km could be applied for this analysis. Although it is true that the smaller the grid cell size, the closer to the representation of exact road surface, there is no difference for the total area of roads in a flood hazard zone in a certain territory. We choose 4 km^2 square cells so that we could accurately represent the roads across the entirety of Switzerland in a series of visually appealing and comprehensible maps. However, it has to be noted that for analyses over irregular areas (i.e. map units) such as states, counties or municipalities, the density of assets should be utilised. Density is calculated by dividing the total exposed area (or assets) of geographic objects by the total area of a corresponding map unit, like a county or municipality. Since we are using equally sized grids, this dividing is not necessary. These initial steps for the flood exposure analysis are indicated in Figure 3, which provides a schematic diagram of the overall operations. The polygons, framed by square cells as depicted in Figure 4, are then used as basic ingredients for developing the following three methods.

4.1. Absolute road area potentially flooded (Method A)

The first method we propose is a direct and absolute approach, often used in the exposure analyses of unlinked assets, such as buildings and cars (Arrighi et al., 2019; Figueiredo and Martina, 2016). This method allows to obtain the absolute amount of exposure, which is an important factor in the calculation of cost benefit analyses of protection measures, which in turn are a condition for allocating public subsidies in many countries (Bründl et al., 2009). Mathematically, our first method consists of summing the area of all the road polygons (i.e. polygons of potentially flood-exposed road segments) within a 4 km^2 square cell:

$$S_F = \sum_i F_i \tag{2}$$

where F_i is the area of a road segment located in a flood hazard zone. The sum S_F is the total area of potentially flooded roads per grid cell, and is calculated for each of the square cells composing the grid. We express the sum S_F in m^2.

4.2. Relative road area potentially flooded (Method B)

The second method considers the relative amount of exposure, which is the ratio of the potentially flooded road area to the total road area, in a square cell. Previously, this method was applied to buildings by (Röthlisberger et al., 2017), for supporting those decision-making processes focused on vulnerability. For our second method of this work, we adapt their approach to roads, by dividing the absolute road area potentially flooded by the total road area in a square cell. The total road surface area S_T of grid cell is

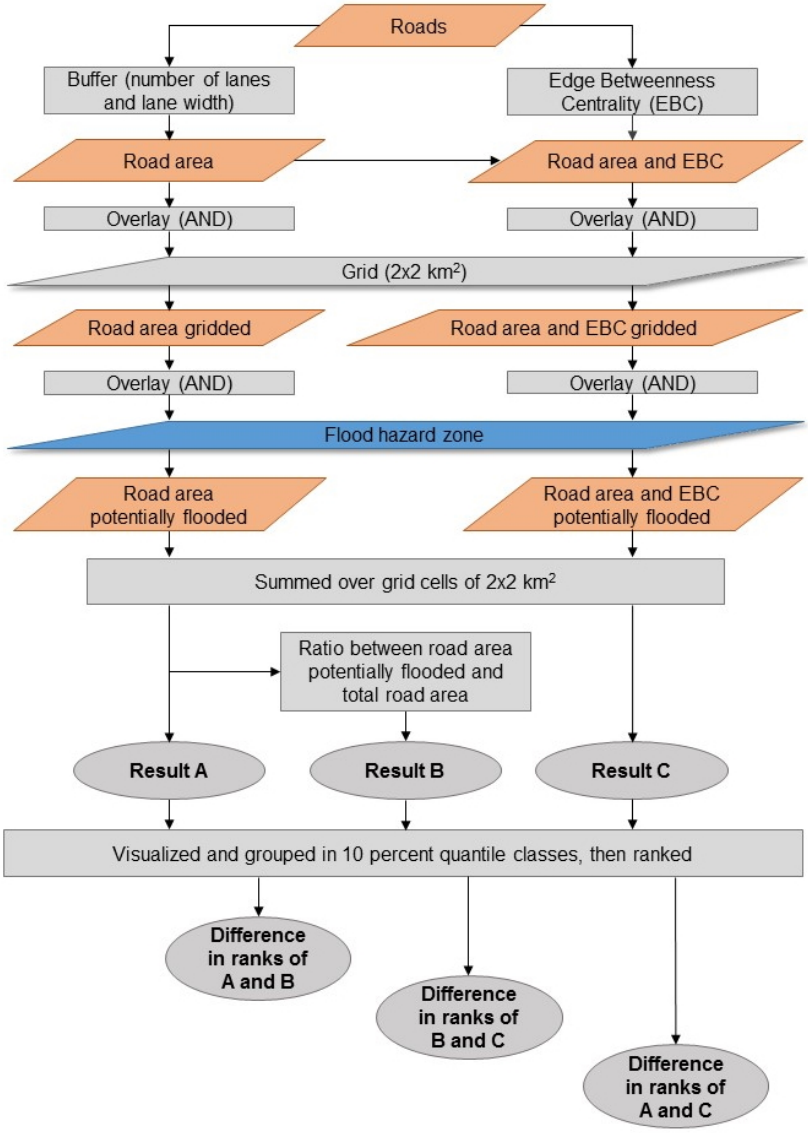

FIGURE 3. Workflow of three methods employed to create difference maps at national level.

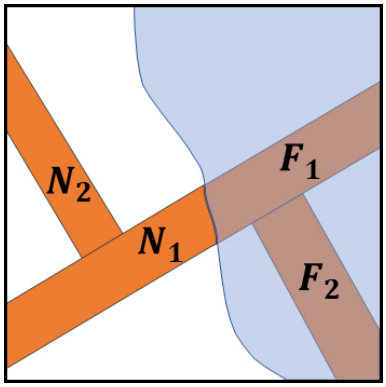

FIGURE 4. Road segment polygons within a grid cell. F_1 and F_2 are in a flood hazard zone (blue area), while N_1 and N_2 are not in any flood hazard zone.

$$S_T = S_F + S_{NF} \tag{3}$$

where S_F is the sum of the road segments' area in a flood hazard zone (Equation 2) and S_{NF} is the total area of road segments that are not located in a flood hazard zone, as shown in Equation 4.

$$S_{NF} = \sum_i N_i \tag{4}$$

where N_i is the surface area of a road segment not located in a flood hazard zone, as shown in Figure 4.

Finally, the ratio is defined as

$$R = \frac{S_F}{S_T}. \tag{5}$$

We obtain the ratio of road areas potentially flooded within a grid cell. The ratio indicates the relative road area in a flood hazard zone within a grid cell.

4.3. Edge betweenness centrality index (EBCI) of absolute road area potentially flooded (Method C)

The third method focuses on the network approach and applies the normalised edge betweenness centrality measure (EBC) that is defined by the number of shortest paths going through an edge (Casali and Heinimann, 2019; Freeman, 1977; Girvan and Newman, 2002), as

$$EBC_E = \frac{1}{N(N-1)} \sum_{s \neq t} \frac{\sigma_{st}(E)}{\sigma_{st}} \tag{6}$$

where σ_{st} is the number of shortest paths from node s to node t, and $\sigma_{st}(E)$ is the number of shortest paths from s to t that pass through edge E, and N is the total number of nodes.

The EBC analysis results in ranking the betweenness centralities of edges (road segments), from the highest to the lowest centrality, according to their connectedness in the network. Edges with higher centrality values have a higher potential to fragment the network into clusters, if they are removed. The EBC analysis can be performed for both unweighted and weighted networks, where the term weighted would refer to features of the edges. In this study, we consider the weight associated to each edge, defining it as the travel time. It is worth mentioning that the EBC analysis of a spatial networks is strongly dependent on the boundary or leaf elements of the network, the so-called "edge effect" or boundary effect according to Okabe and Sugihara (2012), cited in (Gil, 2015). In our road dataset, the road segments are not just weighted, but they have also a direction. Most of the road segments are bidirectional, for which two values of EBC are calculated, while a single EBC value is assigned to the one-directional road segments. The average of these two EBC values is applied for this analysis. Therefore, our EBC calculation is conducted for a weighted and directed network, by using the (Freeman, 1979) and (Brandes, 2001) algorithm, implemented in the igraph module of Python.

The next step is incorporating the betweenness value of an edge or a particular road segment with flood hazard information. Intersecting the roads with grid cells and flood hazard zones, we get many fragmented sections of one road section. In Figure 5, there are F_1, F_2 and F_3 polygons that represent road segments under flood hazard zone and N_1, N_2, N_3, N_4 and N_5 are road segments that are not in any flood hazard zone. Originally, N_1, F_1 and N_5 are one road segment with one EBC assigned. Likewise, N_2, F_2 and N_4 are one road segment with another EBC calculated, and again another EBC is calculated for N_3 and F_3.

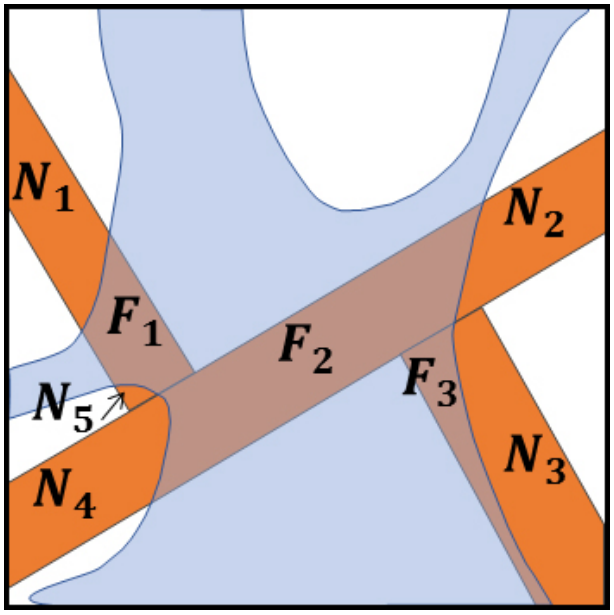

FIGURE 5. Fragmented road segment polygons within a grid cell. F_i are in a flood hazard zone (transparent blue area), while N_i are not in any flood hazard zone.

We then propose to use the same principle of the first presented method (method A), but instead of just calculating the road area potentially flooded within each grid cell, we now assign an EBC value [−] to each road segment and we multiply it by the corresponding road area. The resulting product is summed over all the flooded road segments in a grid cell. We call this sum the edge betweenness centrality index (EBCI) [m^2]·[−].

$$EBCI = \sum_i F_i \times EBC_i. \tag{7}$$

where F_i represents the flood-exposed area of the i-road located in a grid cell, as shown in Figure 4, while EBC_i represents the EBC value of the correspondent i-road.

4.4. Correlation and ranking for comparison

The three methods here presented for assessing flood exposure of roads generate three quantities for each square cell, i.e. S_F, R, and $EBCI$, that we gather in three distinct distributions. Correlation tests are carried out for results of these three methods using Spearman's rank order correlation in R statistical analysis tool. Spearman's correlation test presents the strength of the relationship between two sets of variables. The null hypothesis of Spearman's correlation test is that two variables are not associated.

The alternative hypothesis suggests there is a monotonic relationship that indicates either positive or negative relationship. In the positive relationship when one variable increases the second variable also increases, while in the negative, when one variable increases and the second one decreases. We choose the cut-off value for ρ as 0.7 and -0.7 between strong and weak relationship according to Weaver et al. (2017).

We then use these resulting distributions to compare the three proposed approaches. In particular, we use the statistical concept of quantile. The quantiles are the lines (or cut points) that divide a probability distribution of data into equally sized groups, i.e. with equal probability. In this work, we use 9 quantiles to divide our distributions into 10 equal groups or classes, each of them is called decile (it refers both to the cut-off points and to classes). We use the deciles to assign decile ranks (DR) to our distributed data. The decile rank arranges data derived from the three methods, i.e. road exposure to floods, from lowest to highest on a scale of one to ten. With this decile analysis we identify where the grid cells with the highest ranks of road exposure to floods are located in Switzerland. In Figure 6, the decile ranks are represented by 3 arrays, each one obtained from a single method (A, B and C). The decile classes are reported below each decile rank. In Figure 6, we show the assignment of decile ranks obtained with the three methods, for a representative j-cell. The j-cell has the 8th rank in method A indicating a medium-high exposure level at the national level, while it has 10th rank in method B indicating the highest exposure level. In contrast, this cell has the 5th rank in method C, which indicates a medium-low exposure.

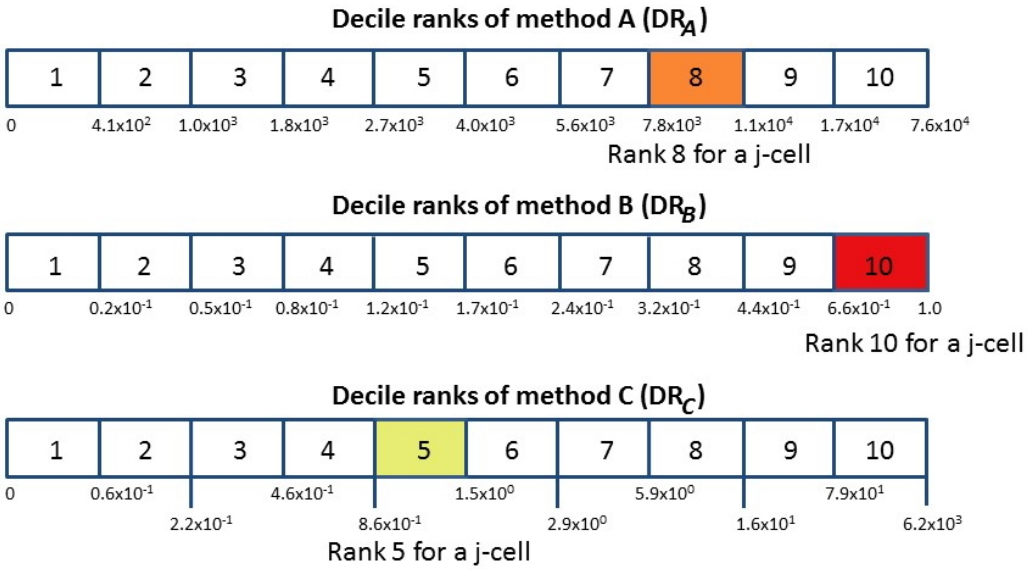

FIGURE 6. Examples of assignment of decile ranks to a j-cell.

The comparison of the resulting distributions is therefore performed by subtracting the decile ranks derived from one distribution from those ones derived from another distribution. We perform this calculation for all the possible combinations, obtaining three maps that we call difference maps. The difference map derived from the difference of deciles ranks of method A and B is shortly indicated by DDR_{A-B}. The difference map between method B and C is shortly indicated by DDR_{B-C} and that one between method A and C is shortly indicated by DDR_{A-C}. The difference maps can have positive or negative values.

In addition to the difference of decile ranks, we also sum up the decile ranks corresponding to the three methods (A, B and C) to obtain the overall exposure to floods at the national level. This result highlights the grid cells with the highest and lowest decile ranks in all three methods.

4.5. Boundary effects in subnetworks

As mentioned in 4.3, the EBC analysis suffers from boundary effects, which could affect some EBC values and ranks. We therefore investigate the impact of the EBC boundary effects on our EBC analysis at national level, by comparing it to the EBCI analysis at a regional level. About the regional level, we consider two subnetworks of the entire Swiss road network: (i) the Cantons of Grisons and Ticino's one and (ii) the Canton of Zurich's one, because of their differences in the density of the regional road network and in their location relative to the boundary of the national network (see Figure 2). We name the regional values of EBCI as $EBCI_r$ and we calculate them for two regional road networks (i) and (ii), separately, after extracting them from the entire Swiss road network (using the same approach mentioned in 4.3).

To compare the regionally calculated $EBCI_r$ with the EBCI that was calculated for the whole country, we use two subsets of EBCI grids reduced to the respective regions and reclassify the two subsets in ten quantile classes each ($EBCI_n$). Then, a difference map, $DDR_{EBCI_n - EBCI_r}$, is created by subtracting the decile rank of newly calculated $EBCI_r$ from the decile rank of $EBCI_n$ per grid. Our analysis on the EBC boundary effects is graphically represented in Figure 7.

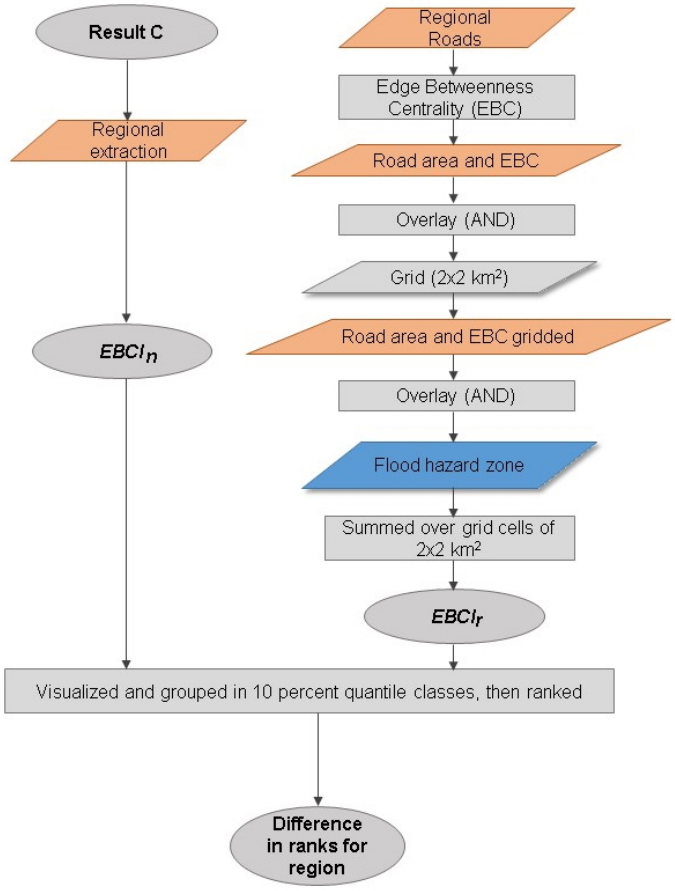

FIGURE 7. Workflow of regional network analysis. It is applied separately both for the Canton of Zurich and the Cantons of Grisons and Ticino

5. Results

In Switzerland, approximately 30 km^2 of major road area (18% of the total major road area) are located in flood hazard zones. While the percentage of potentially flooded road area is similar in the Jura mountains (13%) and in the Swiss Plateau (15%), it is substantially higher (27%) in the Alps (see Table 3). The location of the three biogeographic regions is indicated in Figure 1.

TABLE 3. Major road area statistics by biogeographic regions of Switzerland.

Biogeographic regions	Absolute road area potentially flooded (km^2)	Percent (%)
Alps	13.1	27
Jura	2.8	13
Swiss Plateau	13.7	15
Switzerland	29.6	18

5.1. Road exposure to floods

The results of the three methods for assessing flood exposure of the Swiss roads are presented in Figure 8 i), ii), and iii), respectively: (i) absolute road area potentially

flooded [m^2] (method A), (ii) relative road area potentially flooded [−] (method B), and (iii) EBCI of absolute road area potentially flooded (EBCI) [m^2]·[−]. The left side of this figure comprises maps of the exposure values aggregated in 4 km^2 grid cells with ten quantile classes. The red colouring in the map indicates the highest quantile rank (including the 10% of all grid cells with the highest values), whereas the grids in blue represent the lowest rank of the results of each method. Fig. 8 i) shows that the high ranks (reds) are distributed along the motorways which follow the Alpine rivers (e.g. downstream of Chur along the Rhein valley and of Sion in the Rhone valley) and around some large Swiss cities, such as Zurich, Lucerne, Bern, and Yverdon-Les-Bains. The areas along motorways are highly populated, with major roads developed within the floodplains of major rivers. The areas around large Swiss cities are obviously highly urbanized regions with high road density (see Fig. 1 and 2). Thus, red grid cells indicate areas with both vast flood hazard zones and road areas. In contrast, low absolute exposure (blueish colour) of the road network appears in the rural areas of the Swiss Plateau and in the Alps, with the exception of the flood-exposed road network in the main valleys. On the right, the distribution plots show that grid cells in the Swiss Plateau indicate the highest peaks of low values, followed by the Alps. The distribution of the Jura region differs slightly from the other two regions. In all three regions, grid cells with exposure values above 25 000 m^2 are limited.

TABLE 4. Mean values of results of methods A, B, and C per biogeographic regions of Switzerland (see Table 3). The location of the three biogeographic regions is indicated in Figure 1, section 3.2

Biogeographic regions	mean of A (m^2)	mean of B (0-1)	mean of C
Alps	7589.9	0.33	58.68
Jura	5654.1	0.24	31.52
Swiss Plateau	6830.2	0.20	52.42

The left side of Fig. 8 ii) exhibits red grid cells with a high ratio of flood exposed road segments. These grid cells are located in or near smaller cities such as Martigny in the Rhone river valley or Buchs in the Rhine river valley. Furthermore, grid cells in most valleys of the Swiss Alps that have one or few main road connections to a head valley are classified as higher ranks. We can recognize mountainous areas with high ratios distinctly from lower or medium ratio areas in the Swiss Plateau. For instance, and in contrast to the results of method A, the city of Zurich is not distinguishable in result B. The mean values in method B (Table 4) show the value in the Alps to be substantially higher than the mean values of the other two regions. This is confirmed by the distribution plots on the right side of Figure 8, which show the highest peak of the distribution is the lowest for the Swiss Plateau, followed by the Jura region. The grid cells in the Alps have more high ratio values than the other two regions.

The left side of Fig. 8 iii) indicates high exposure to floods along highways allowing fast travel speed. Higher ranks are related to the increased connectivity of main links of the network. The most exposed connections are the highway between Solothurn and Aarau, the highway connecting the cantons Valais and Vaud, the roads between Valais and Ticino, the highway connecting the city of Lucerne to the Canton of Ticino, and the highway along Rhine river valley. Compared to methods A and B, method C emphasizes the main road network. While mean values are very similar in the Alps

and Swiss Plateau (Table 4), the mean value of the Jura region is half of the other two regions.

On the right side of Figure 8, the distributions of the exposure values are presented, which are differentiated by the three biogeographic regions indicated in Figure 1. For all three methods and for all three regions, the distributions (Fig. 8, right side) of the exposure values per grid cell are right-skewed (it has to be noted that the distribution of method C has been log transformed), indicating that the majority of the grid cells have values lower than the mean values (see Table 4 for the mean values). They all have one peak in the lower end of the values suggesting most of the grid cell values have low values and few values with high values. For the method A and C, distributions of the three biogeographic regions are almost overlapping suggesting their frequencies are similar. However, in method B, the distributions are distinct for each biogeographic region; the Alps have more high ratio grid cells than other two regions.

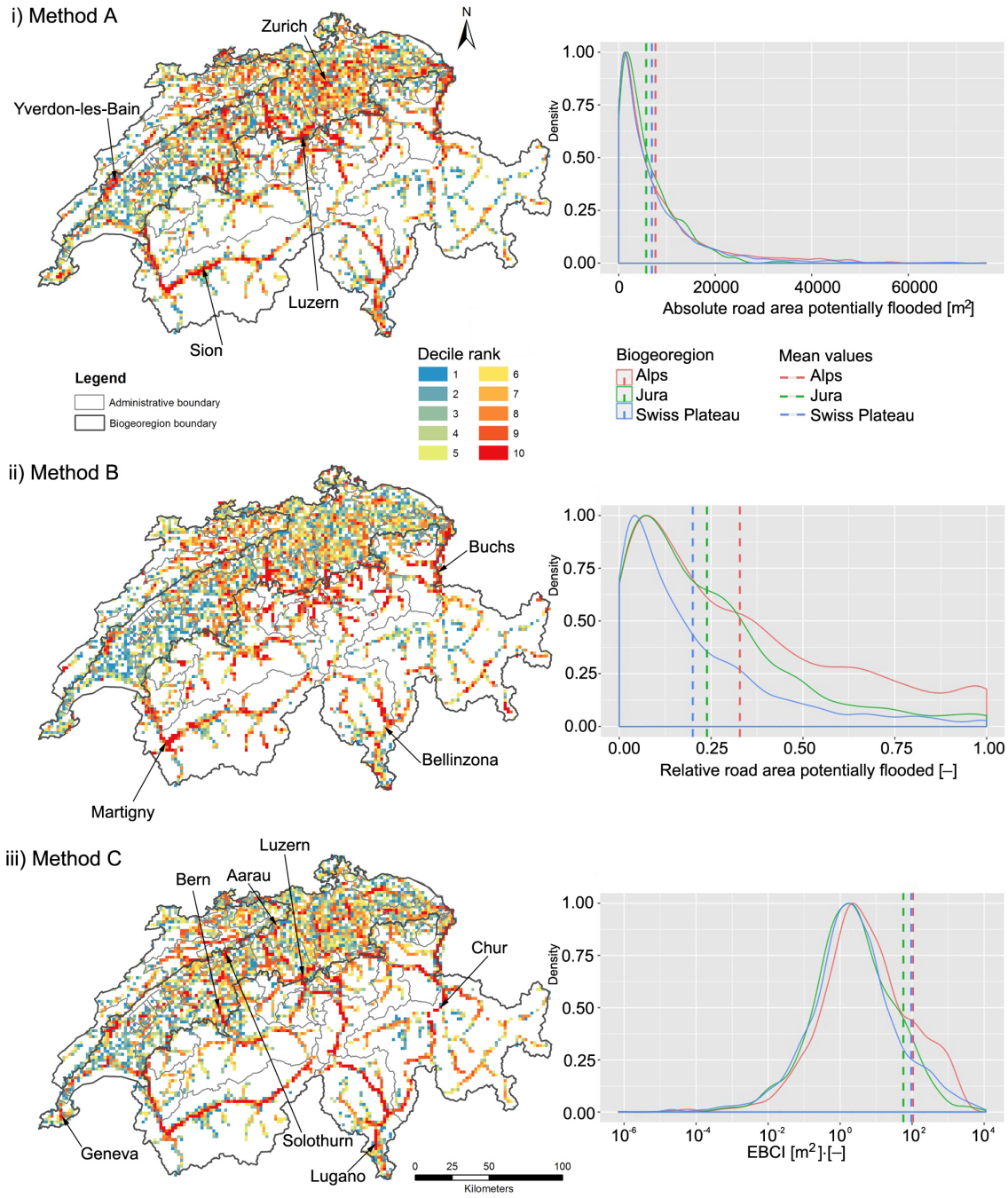

FIGURE 8. On the left, results of three different methods for flood exposure aggregated and then ranked. On the right, distribution plots of various exposure values according to each method by biogeographic regions. X axis for method C is log transformed.

5.2. Comparison between the three proposed methods

To analyse the correlation of the results of the three methods we apply the Spearman's rank order correlation test, since the pairwise scatterplots indicate monotonic relationships. Spearman's rank correlation test results are presented in Table 5.

TABLE 5. Correlation tests between results of methods A, B and C.

Methods	Spearman's rank correlation	p-value
A and B	$\rho = 0.77$	$< 2.2e-16$
A and C	$\rho = 0.74$	$< 2.2e-16$
B and C	$\rho = 0.55$	$< 2.2e-16$

There are positive correlations between results from Methods A and B ($\rho = 0.77, p < 2.2e-16$), results from Methods A and C ($\rho = 0.74, p < 2.2e-16$), and results from Methods B and C ($\rho = 0.55, p < 2.2e-16$). The relationships between A and B, and A and C are strong and similar, at 0.77 and 0.74, respectively. When rank of A increases, rank of B increases, although the relationship is not perfect monotonic. The same pattern holds also for the correlation between A and C. In contrast, the relationship between B and C is weak, at 0.55, and almost one third lower than the other two. Therefore, differences between the results are quantified.

The comparison of the three methods' results is shown in Figure 9, by illustrating the differences among the decile ranks calculated with each method: i) rank of absolute road area potentially flooded – rank of relative road area potentially flooded; ii) rank of relative road area potentially flooded – rank of edge betweenness centrality index of absolute road area potentially flooded; iii) rank of absolute road area potentially flooded – rank of edge betweenness centrality index of absolute road area potentially flooded. Roughly speaking, we show whether the decile rank of a grid resulting from one method is higher than, equal to, or lower than the decile rank resulting from another method. There are total of 4283 grid cells of 2 km by 2 km area having roads in flood hazard zones in Switzerland. The differences are presented in maps on the left side of Figure 9, and as scatterplots on the right side. We characterise the entire Figure 9 with three colours: Grey to indicate no or little difference between two ranks (namely a maximum difference of one rank); blue to symbolise a rank at least two decile ranks higher in the first method (e.g., DR_A in DDR_{A-B}) than in the second method (e.g., DR_B in DDR_{A-B}); and red to symbolise a rank at least two decile ranks lower.

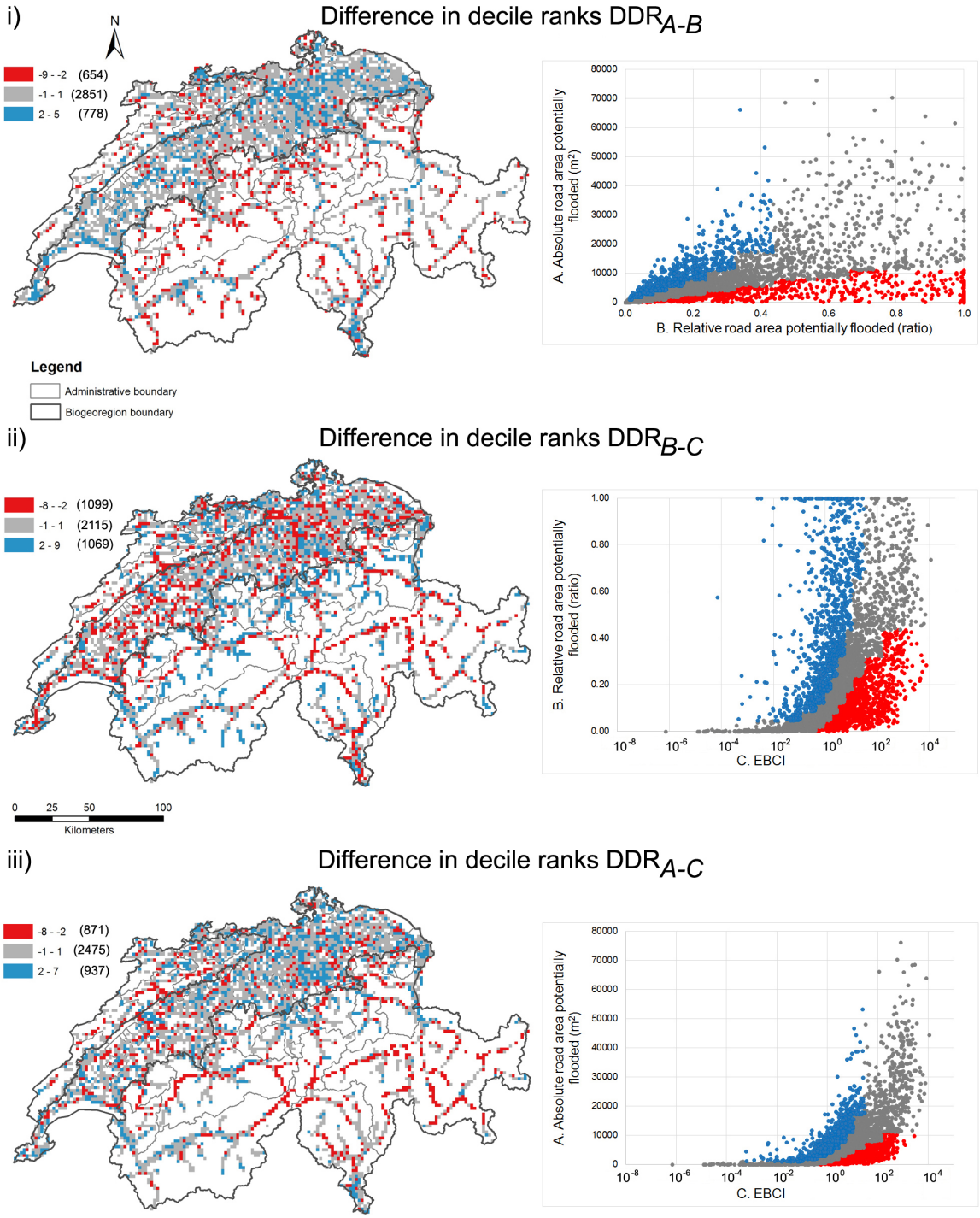

FIGURE 9. On the left, pairwise difference maps of ranks per 4 km^2 grid cells. On the right, pairwise differences in ranks are shown by scatterplots. Red: difference is equal to -2 or lower; Grey: difference is between (and included) -1 and 1; Blue: difference is equal to 2 or higher.

Overall, we observe that grey grid cells, indicating little or no difference between the quantile ranks of methods A and B, dominate the entire Figure 9 i), outnumbering the coloured grid cells (which indicate a difference of at least two quantile ranks) by 3.6 times. For cases DDR_{B-C} and DDR_{A-C}, the grey cells are less pronounced than

the coloured ones, being, respectively 2 and 2.6 times more numerous. The spatial distribution of the grey cells does not show a clear pattern.

Figure 9 i) DDR_{A-B} presents the difference between the ranks of absolute road area potentially flooded (method A) and the ranks of the ratio approach (method B). The blue grid cells (where DR_A is at least two quantile ranks higher than DR_B) are clustered in the Swiss Plateau. These grid cells indicate highly urbanized regions with large potentially flooded road areas, which however only represent a low share of the regions' total road areas. In contrast, the red grid cells are mainly located in the mountainous regions. These grid cells represent regions with high values in method B but low values in method A. The low absolute value of potentially flooded road areas (method A) is predominantly due to a low road density in these mainly rural areas. On the right side of Figure 9 i), the scatterplot of A and B quantile ranks indicates that blue grid cells' values in method B does not exceed 0.44. In contrast, red cells values in method A is below 11 560 m^2. The grey coloured cells show the highest spread of exposure values of both methods which increases with the rising exposure values.

Figure 9 ii) DDR_{B-C} shows the differences between ranks of method B (ratio of potentially flooded road areas) and method C (EBCI of the absolute road areas potentially flooded). The coloured grids both show a weak spatial pattern within the Alps. The blue grids are noticeably frequent in remote Alpine valleys. They indicate regions with a high ratio of potentially flooded road areas (method B) but a comparatively low EBCI (method C). This low EBCI in remote Alpine valleys results from (i) a low road density and (ii) a low importance of these roads within the national road network. In contrast, the red grid cells are frequent along Alpine transit routes. These cells represent areas with comparatively low values in method B but high EBCI values, the latter indicating large road areas both potentially flooded and important for the connectedness of the national road network. On the right side of Figure 9 ii), the scatterplot of B and C quantile ranks shows that the red grid cells' values for the relative road area potentially flooded (method B) are lower than 0.44 and EBCI are higher than 0.39. In contrast, blue cells have only values of EBCI that are lower than 16.6.

Figure 9 iii) DDR_{A-C} presents the difference between ranks of method A (absolute road area potentially flooded) and method C (EBCI absolute road area potentially flooded). As in the previous two cases (DDR_{A-B}, DDR_{B-C}) the majority of the grids are grey, and these grey grid cells are not spatially clustered. In contrast, the blue grids are clustered in the Swiss Plateau, though the clustering is less pronounced than in the DDR_{A-B} difference. These blue grid cells in the Swiss Plateau represent densely urbanized regions with large potentially flooded road areas but comparatively low EBCI, indicating that the potentially flood-prone road areas of these regions are of minor importance for the national road networks' connectedness. The red grid cells again are remarkably frequent along Alpine transit routes. They indicate regions where the potentially flooded road areas are comparatively small (method A) but these potentially flooded roads are important for the national road network (method C). On the right side of Figure 9 iii), the scatterplot of A and C decile ranks indicates that the values of blue grid cells in the network approach does not exceed 16.1, while red cells' values in method A do not exceed 10000.

Figure 10 shows histograms of the pairwise differences. Figure 10 i) presents the histogram of difference in decile ranks of method A and method B, (DDR_{A-B}) which is slightly left-skewed. This histogram has more positive values (i.e. 778 blue cells) than

negative values (654 red cells), indicating that the number of grid cells with a higher rank in A than in B exceeds the number with a lower rank in A than in B. In Figure 10 ii) the histogram of difference in decile ranks of B and C (DDR_{B-C}) is approximately equally distributed both in right and left sides, indicating that the numbers of grid cells that have higher ranks and lower ranks are similar. In Figure 10 iii), the histogram of difference in decile rank of method A and method C (DDR_{A-C}) is approximately equally distributed in right and left sides, indicating that the numbers of grid cells that have higher ranks and lower ranks are similar.

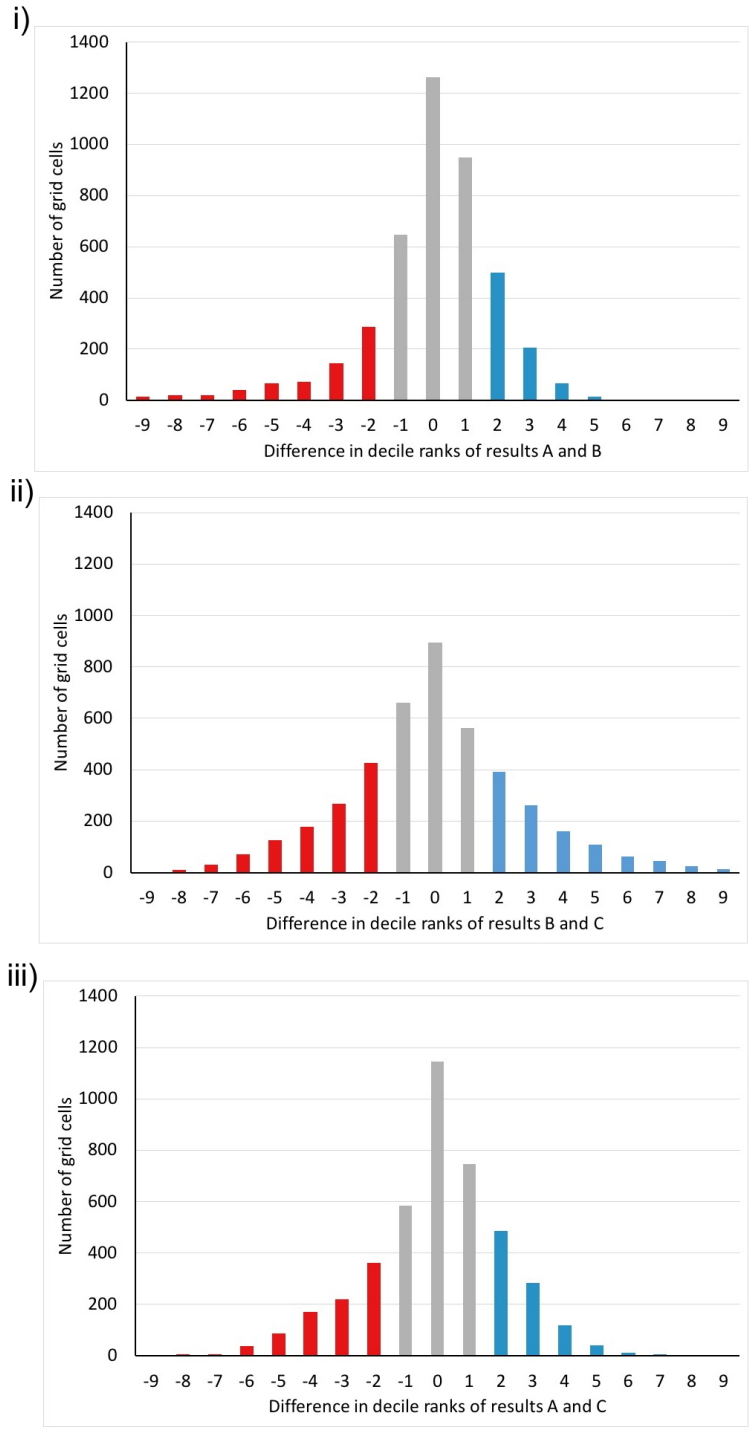

FIGURE 10. Histograms of the differences in decile ranks of results for grid cells.

The overall flood-exposure map at the national level is presented in Figure 11. The map shows the total of ranks from all three methods and it indicates areas that have the highest rank in each method in red (higher values in reddish), the lowest rank in each method in blue (lower values in blueish), whereas areas with medium levels of overall flood exposure (values of 6-27) are presented in white. Red or reddish cells indicate

areas where the flood exposure of roads is high, regardless of the method chosen. These areas are commonly in major river valleys.

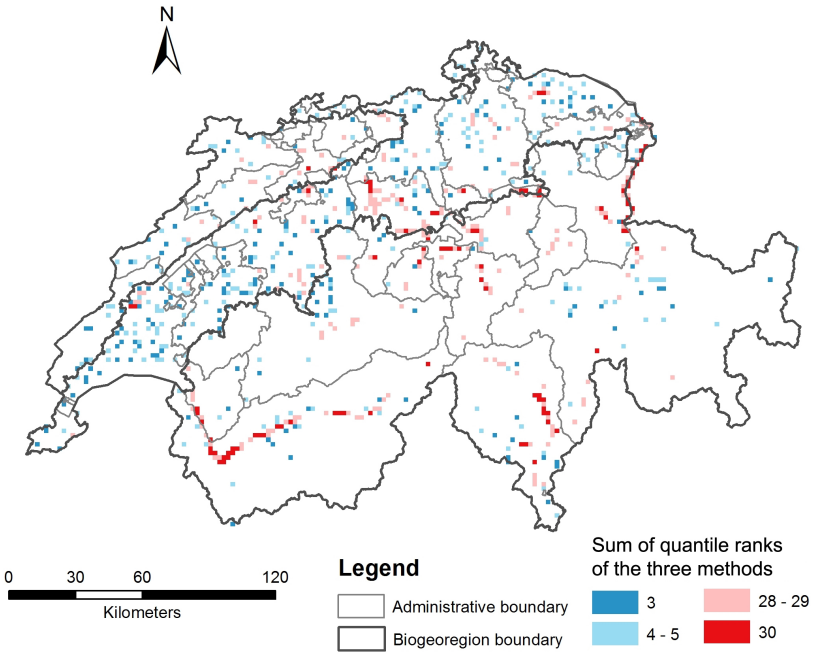

FIGURE 11. Total of ranks from each method ($DR_A + DR_B + DR_C$).

5.3. Comparison of national and regional network

Figure 12 and 13 present the results of the two regional analysis with method C (EBCI) compared to the results of the same method at national level. Figure 12 indicates that flood-exposed roads in the north of the Grisons and Ticino area are important in the national network but are less important in the regional network, which is indicated by the blue cells in the difference map. In contrast, the potentially flooded roads in the southern part connecting Bellinzona and Chur, the road between St. Moritz and Zernez, and the road connecting Tiefencastel and Davos are more important (red cells) in the regional network. Thus, the difference map of the national and regional road networks highlights how the rank of exposure to floods within the grid cells changes depending on the network's extent. Thus, the boundary effect is well illustrated within the EBCI approach.

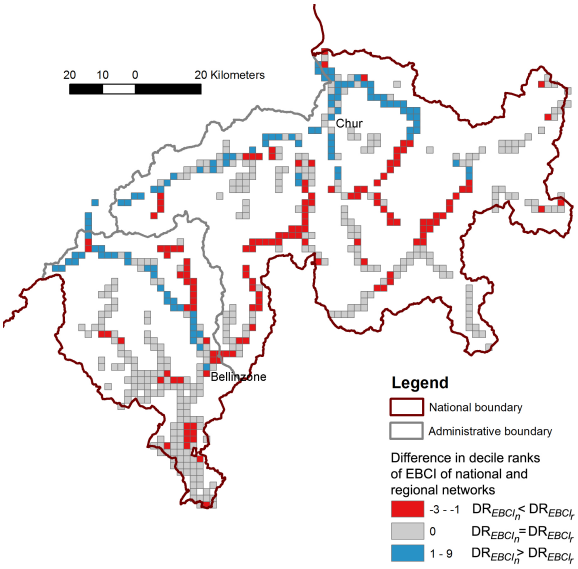

FIGURE 12. Difference of ranks between $EBCI_n$ and $EBCI_r$ in regional network in the Cantons of Grisons and Ticino

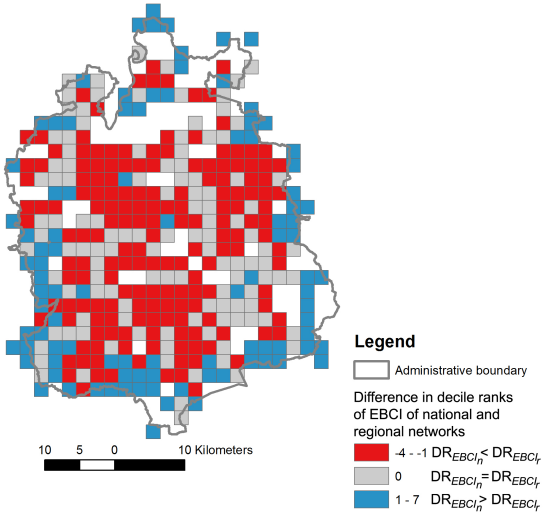

FIGURE 13. Difference in decile ranks between $EBCI_n$ and $EBCI_r$ in regional network in the Canton of Zurich

In contrast to the results in the peripheral Cantons Grison and Ticino, the results for the central and highly urbanised Canton of Zurich (Figure 13) indicate for the roads along the regional boundary lower ranks of $EBCI_r$ than $EBCI_n$. The grid cells along the regional boundary actually have higher $EBCI_n$ values because they are closely connected to the surrounding regions. Considering the regional network, almost all the grid cells in the central part resulted in the difference map with higher $EBCI_r$ values and thus higher ranks since the roads are closely connected to each other by a lattice-like (Tsiotas, 2017) road structure (see Figure 13).

6. Discussion

The results of all three methods present exposure to floods but in significantly different ways. The application of methods A and B needs only a few simple GIS functions and thus, low computation time to consider the national level in Switzerland. However, exposure analysis using these two approaches could also be challenged by data availability (Narayanan et al., 2016), homogeneity, and comparability of data quality, as Qiang (2019) observed when considering flood exposure in the U.S. In contrast to the low computation time of method A and B, method C, depending on the size and level of detail of the road networks with possible millions of road segments, requires more computation time and resource.

Method A indicates the spatial distribution of the quantity of road areas that could be flooded in Switzerland. The general pattern of the exposure of roads to flooding follows the characteristics of biogeographic regions, as expected. In the Alps, most of the roads that show a high flood exposure according to method A follow main river valleys, such as along the Rhone and Rhine river valleys, because in the floodplain flat space was available and allowed the road infrastructure to develop further in a cost-efficient way, especially after first flood protection (see Figure 2). In contrast, the road pattern is lattice-like in the Swiss Plateau, since the topography of this region is generally flatter and allowed a greater spread of urban development and related road infrastructure. These regions (e.g. Zurich, Lucerne, Yverdon-Les-Bains) have a large quantity of flood-exposed road areas. And this quantity is a magnitude of order higher in the Swiss Plateau than in the two other regions. In general, the results of method A are driven by the higher quantity of roads built in flood hazard zones. This method is not sensitive to the road network extent, meaning the boundary of the study area does not influence the results. This method indicates reconstruction costs in case of flood-induced damages. Furthermore, the results provide risk managers with information on where to make priority decisions for more detailed risk assessments. Comparing the statistical distribution of the results of method A in the three biogeographic regions, we recognize three similar patterns: the most of the low values are below the mean, the mean values are close to each other and number of grid cells with high exposure values is limited.

The relative road area potentially flooded, method B, highlights lateral mountain valleys in the Alps that have few access roads, and these roads are in flood hazard zones. For the population living in these valleys, one of the means of transport is under threat, thus revealing local areas of Switzerland vulnerable to flooding. In addition, cities such as Sion and Martigny are located in main valleys, and results for these valleys indicate high ranks of relative road areas at risk of flooding. In contrast, values in the city of Zurich are not higher than in the 8th decile rank (see Figure 8 ii). Compared to the top ranked lateral mountain valleys, Zurich and other cities in the Swiss Plateau are less vulnerable, because there are alternative roads that can be used in the event of flooding. Method B is not sensitive to the road network extent, implying that this method will present similar results if the network's boundaries are changed. The exposure identified by method B provides more information about possible decreased accessibility during a flood event. This information can be used for risk management decisions on prevention investments for certain areas or on organizing preparedness measures for possibly affected communities. The statistical distributions of the results of method B show remarkable differences between the three biogeographic regions of Switzerland.

The alpine region has a substantially higher number of grid cells with high exposure values than the two other regions, which is reflected in a higher mean value too.

The results of the EBCI (method C) present the network's most connected roads that are in flood hazard zones. Compared to the other methods, the network approach emphasizes the importance of possibly flooded road segments. Applied to risk management, the results of method C support decisions focused on the connectivity and thus functionality of a road network during an event. Areas with high ranks in method C and method B are dominant in the Swiss Alps. Similarly to a study by Erath et al. (2009), the EBCI is categorised as a system-based approach according to Mattsson and Jenelius (2015). However, our study differs from the one by Erath et al. (2009), as we develop a spatial explicit EBC index rather than an abstract network. Moreover, the boundary effects mentioned by Gil (2015) are presented clearly in the comparison of the $EBCI_n$ and $EBCI_r$. This comparison suggests that the comparability between regional and national level flood exposure studies is limited. Even at the national level alone, the boundary effects are relevant, as the analysed road network is limited to the national border and does not continue to the surrounding countries. This raises the question of where the road network extent should end for national-level analyses. This limitation should be addressed in future studies. The statistical distributions of the decile ranks in the three biogeographic regions are similar with the following exceptions: The mean value of the Jura is clearly lower than in the two other regions and the Alps have a remarkably higher number of grid cells with high exposure values than the Jura mountains or the Swiss Plateau.

Even though there are differences in the spatial patterns of the three methods, there are also areas where all three methods present similar results. The strong positive relationships between the methods A and B, and A and C mirror the involvement of road area potentially flooded. Nevertheless, the correlation between B and C is weak and it suggests much more differences between these two methods. The areas with the highest flood-exposure of roads indicated in red are mainly in major river valleys, predominantly in the Alps (see Figure 11). Independently of the method applied, the results for these alpine river valleys suggest a high exposure of roads to floods. For flood risk management, this implies prioritizing measures in these areas regardless of the focus of the risk management strategy. In contrast, the lowest flood-exposed areas in all three methods are presented in blue and they are mainly in the Swiss Plateau.

The result of the flood exposure analysis indicates road sections that could possibly be flooded but it is crucial to highlight that this cannot happen all at the same time. However, the overall exposure information is important for decision-making and risk management to identify the potentially flooded road sections, to address risk reduction measures and event management strategies. Thus, in this case the spatial pattern of flood exposure on a national level is very important. Due to the different responsibilities of hazard and risk management on federal, cantonal (including 26 states) and municipal level, compiled hazard maps at a national level are missing, and thus a nationwide overview for prioritization, and consequently coordination between the different states and municipalities, needs to be improved. Using the compiled national flood hazard map, it was possible to conduct this national exposure analysis on a very detailed level, and to address the research questions on exposure pattern. Although a flood event could happen in a particular area of the country at any moment, national level exposure analysis enables a comparison of exposure levels between biogeographic

regions of Switzerland. Considering the size of Switzerland (41285 km^2), the study could perhaps be transferred or compared to other countries as a regional study on flood exposure.

7. Conclusion

Analysis of road infrastructure exposure to flooding is a first and important step for risk analysis. However, most of the previous studies include this examination into the vulnerability and/or consequence analysis. Exposure analysis can provide crucial information for decision making on where to prioritise risk reduction measures on road infrastructure. This study demonstrates the importance of an appropriate choice of methods in flood exposure analysis. We develop and apply three methods to assess the flood exposure of the road infrastructure: absolute road area potentially flooded (method A), relative road area potentially flooded (method B), and network-based approach using the edge betweenness centrality index (EBCI, method C). All three methods are applied to the major road infrastructure of Switzerland (national level) and visualized by grid cells of 2 km by 2 km. Results of the methods present distinct spatial patterns; grid cells with higher ranks in method A indicate where high quantity of road areas are in flood hazard zones (urban or high road density areas in flood plains), so the results are strongly influenced by the density of road network, while grid cells with higher ranks in method B indicate areas having a high ratio of the potentially flooded road area to the total road area. Most of them are in the mountainous areas of Switzerland. In contrast to method A, method B allows to distinguish major biogeographic regions in the study area indicating infrastructure development pattern following geographical conditions. Both Method A and B are not sensitive to the road network boundary. Higher ranks in method C, the edge betweenness centrality index, present the most-connected potentially flooded road links within a boundary of network. Compared to the other two methods, this approach demands longer computation time and exhibits higher dependency on data availability, and on the setting of a network extent due to the boundary effect. However, method C offers a new way of flood exposure assessment taking into account the whole system as a network. Most of the grid cells that have higher decile ranks in ratio (method B) than edge betweenness centrality index (method C) indicate isolated mountain valleys that can only be accessed by a single road. The access roads to these valleys need to be investigated further for flood vulnerability analysis in Switzerland. The next logical step would be to analyse the direct and indirect consequences of flooding a road segment to better understand the effects of partial or complete blockage on traffic. In any case, there is no "one size fits all" method to assess the exposure of roads to floods. The method and extent of an exposure analysis must fit to the focus of the risk management decisions which the analysis informs.

Acknowledgements: We thank the natural hazards group at the Swiss Mobiliar Insurance Company "die Mobiliar AG" for acquiring and compiling the communal flood hazard maps. We also thank the Federal Office for Spatial Development (ARE) for providing the major road network data.

References

Agryzkov, T., Oliver, J.L., Tortosa, L., Vicent, J., 2014. A new betweenness centrality measure based on an algorithm for ranking the nodes of a network q. APPLIED MATHEMATICS AND COMPUTATION 244, 467–478. URL: http://dx.doi.org/10.1016/j.amc.2014.07.026, doi:10.1016/j.amc.2014.07.026.

ARE, 2016. Nationales Personen- und Güterverkehrsmodell des UVEK – Durchschnittlicher Tagesverkehr 2015 für den Personen- und Güterverkehr auf Strasse und Schiene. Technical Report. Federal Office for Spatial Development ARE (Bundesamt für Raumentwicklung).

Arrighi, C., Pregnolato, M., Dawson, R.J., Castelli, F., 2019. Preparedness against mobility disruption by floods. Science of the Total Environment 654, 1010–1022. URL: https://doi.org/10.1016/j.scitotenv.2018.11.191, doi:10.1016/j.scitotenv.2018.11.191.

Balijepalli, C., Oppong, O., 2014. Measuring vulnerability of road network considering the extent of serviceability of critical road links in urban areas. Journal of Transport Geography 39, 144–155. doi:10.1016/j.jtrangeo.2014.06.025, arXiv:ISSN 0966-6923.

Berdica, K., 2002. An introduction to road vulnerability: What has been done, is done and should be done. Transport Policy doi:10.1016/S0967-070X(02)00011-2.

Birkmann, J., Welle, T., 2015. Assessing the risk of loss and damage: exposure, vulnerability and risk to climate-related hazards for different country classifications. International Journal Global Warming 8, 191–212.

Borter, P., 1999. Risikoanalyse bei gravitativen Naturgefahren Methode. umwelt-mat ed. Bundesamt für Umwelt, Wald und Landschaft (BUWAL). https://www.bafu.admin.ch/bafu/de/home/themen/naturgefahren/publikationen-studien/publikationen/risikoanalyse-gravitativen-naturgefahren.html.

Brandes, U., 2001. A Faster Algorithm for Betweenness Centrality. Journal of Mathematicl Sociology 25, 163–177.

Bründl, M., Romang, H.E., Bischof, N., Rheinberger, C.M., 2009. The risk concept and its application in natural hazards risk management in Switzerland. Natural Hazards Earth System Sciences 9, 801–813.

Cabinet Office, 2010. Strategic Framework and Policy Statement on Improving the Resilience of Critical Infrastructure to Disruption from Natural Hazards.

Casali, Y., Heinimann, H.R., 2019. A topological analysis of growth in the Zurich road network. Computers, Environment and Urban Systems 75, 244–253. doi:10.1016/j.compenvurbsys.2019.01.010.

Chiaradonna, S., Giandomenico, F.D., Lollini, P., 2008. Evaluation of Critical Infrastructures: Challenges and Viable Approaches. volume 5135. Springer, Berlin, Heidelberg.

Coppola, D.P., Coppola, D.P., 2015. Recovery. Introduction to International Disaster Management , 405–460URL: https://www.sciencedirect.com/science/article/pii/B9780128014776000071, doi:10.1016/B978-0-12-801477-6.00007-1.

Costa, L.d.F., Rodrigues, F.A., Travieso, G., Boas, P.R.V., 2007. Characterization of complex networks: A survey of measurements. Advances in Physics 56, 167–242.

Debionne, S., Ruin, I., Shabou, S., Lutoff, C., Creutin, J.D., 2016. Assessment of commuters' daily exposure to flash flooding over the roads of the Gard region, France. Journal of Hydrology 541, 636–648.

Demšar, U., Špatenková, O., Virrantaus, K., 2008. Identifying Critical Locations in a Spatial Network with Graph Theory. Transactions in GIS 12, 61–82.

Erath, A., Birdsall, J., Axhausen, K.W., Hajdin, R., 2009. Vulnerability Assessment Methodology for Swiss Road Network. Transportation Research Record 2137, 118–126.

European Commission, 2005. Green Paper on a European Programme for Critical Infrastructure Protection. COM(2005) 576 Final, Brussels, Belgium.

Federal Office for the Environment, 2008. Aquaprotect. URL: https://www.bafu.admin.ch/bafu/de/home/themen/naturgefahren/fachinformationen/naturgefahrensituation-und-raumnutzung/gefahrengrundlagen/aquaprotect.html.

Federal Office of Topography, 2017. swissBOUNDARIES3D. https://shop.swisstopo.admin.ch/en/products/landscape/boundaries3D. URL: https://shop.swisstopo.admin.ch/en/products/landscape/boundaries3D.

Figueiredo, R., Martina, M., 2016. Using open building data in the development of exposure data sets for catastrophe risk modelling. Natural Hazards and Earth System Sciences 16, 417–429.

Freeman, L., 1979. Centrality in Social Networks' Conceptual Clarification. Social Networks 1, 215–239.

Freeman, L.C., 1977. A Set of Measures of Centrality Based on Betweenness. Sociometry 40, 35. URL: http://www.jstor.org/stable/3033543?origin=crossref, doi:10.2307/3033543.

Fuchs, S., Keiler, M., Sokratov, S., Shnyparkov, A., 2013. Spatiotemporal dynamics: The need for an innovative approach in mountain hazard risk management. Natural Hazards 68, 1217–1241. doi:10.1007/s11069-012-0508-7.

Fuchs, S., Keiler, M., Zischg, A., 2015. A spatiotemporal multi-hazard exposure assessment based on property data. Natural Hazards and Earth System Sciences 15, 2121–2142.

Gheorghe, A.V., Masera, M., Weijnen, M., Vries, L.J.D., 2006. Critical Infrastructures at Risk: Securing the European Electric Power System. Topics in Safety, Risk, Reliability and Quality.

Gil, J., 2015. Examining 'edge effects': Sensitivity of spatial network centrality analysis to boundary conditions, in: SSS10 (Ed.), Proceedings of the 10th International Space Syntax Symposium.

Girvan, M., Newman, M.E.J., 2002. Community structure in social and biological networks. Proceedings of the National Academy of Sciences of the United States of America 99, 7821–7826. doi:10.1073/pnas.122653799, arXiv:0112110.

Graham, S., 2009. Disrupted Cities: When Infrastructure Fails. 1 ed., Routledge.

Hankin, B., Craigen, I., Rogers, W., Morphet, J., Bailey, A., Whitehead, M., 2016. Flood Risk to the Strategic Road Network in England. E3S Web of Conferences 7, 10001. URL: http://www.e3s-conferences.org/10.1051/e3sconf/20160710001, doi:10.1051/e3sconf/20160710001.

Hanslow, D.J., Morris, B.D., Foulsham, E., Kinsela, M.A., 2018. A Regional Scale Approach to Assessing Current and Potential Future Exposure to Tidal Inundation in Different Types of Estuaries. Scientific Reports 8, 1–13. URL: http://dx.doi.org/10.1038/s41598-018-25410-y, doi:10.1038/s41598-018-25410-y.

Helderop, E., Grubesic, T.H., 2019. Flood evacuation and rescue: The identification of critical road segments using whole-landscape features. Transportation Research Interdisciplinary Perspectives 3, 100022. URL: https://doi.org/10.1016/j.trip.

2019.100022, doi:10.1016/j.trip.2019.100022.

Hirabayashi, Y., Mahendran, R., Koirala, S., Konoshima, L., Yamazaki, D., Watanabe, S., Kim, H., Kanae, S., 2013. Global flood risk under climate change. Nature Climate Change 3, 816–821. doi:10.1038/nclimate1911.

Hu, X., Hall, J.W., Shi, P., Lim, W.H., 2016. The spatial exposure of the Chinese infrastructure system to flooding and drought hazards. Natural Hazards 80, 1083–1118. doi:10.1007/s11069-015-2012-3.

Jenelius, E., Mattsson, L.G., 2015. Road network vulnerability analysis: Conceptualization, implementation and application. Computers, Environment and Urban Systems 49, 136–147.

Jenelius, E., Peterson, T., Mattsson, L.G., 2006. Importance and exposure in road network vulnerability analysis. Transportation Research Part A 40, 537–560.

Jongman, B., Kreibich, H., Apel, H., Barredo, J.I., Bates, P.D., Feyen, L., Gericke, A., Neal, J., Aerts, J.C.J.H., Ward, P.J., 2012a. Comparative flood damage model assessment: towards a European approach. Natural Hazards and Earth System Sciences 12, 3733–3752.

Jongman, B., Ward, P.J., Aerts, J.C., 2012b. Global exposure to river and coastal flooding: Long term trends and changes. Global Environmental Change 22, 823–835. URL: http://dx.doi.org/10.1016/j.gloenvcha.2012.07.004, doi:10.1016/j.gloenvcha.2012.07.004.

Kappes, M.S., Gruber, K., Frigerio, S., Bell, R., Keiler, M., Glade, T., 2012. The MultiRISK platform: The technical concept and application of a regional-scale multihazard exposure analysis tool. Geomorphology 151-152, 139–155. URL: http://dx.doi.org/10.1016/j.geomorph.2012.01.024, doi:10.1016/j.geomorph.2012.01.024.

Kermanshah, A., Derrible, S., Berkelhammer, M., 2017. Using climate models to estimate urban vulnerability to flash floods. Journal of Applied Meteorology and Climatology 56, 2637–2650. doi:10.1175/JAMC-D-17-0083.1.

Kulp, S., Strauss, B.H., 2017. Rapid escalation of coastal flood exposure in US municipalities from sea level rise. Climatic Change 142, 477–489. doi:10.1007/s10584-017-1963-7.

Kundzewiz, Z.W., Kanae, S., Seneviratne, S.I., Handmer, J., Nicholls, N., Peduzzi, P., Mechler, R., Bouwer, L.M., Arnell, N., Mach, K., Muir-Wood, R., Brakenridge, G.R., Kron, W., Benito, G., Honda, Y., Takahashi, K., Sherstyukov, B., 2014. Flood risk and climate change: global and regional perspectives. Hydrological Sciences Journal 59, 1–28. doi:10.1080/02626667.2013.857411.

Kunz, M., Hurni, L., 2008. Hazard Maps in Switzerland: State-of-the-Art and Potential Improvements. 6th ICA Mountain Cartography Workshop Mountain Mapping and Visualization .

Loat, R., Petrascheck, A., 1997. Berücksichtigung der Hochwassergefahren bei raumwirksamen Tätigkeiten.

Mattsson, L.G., Jenelius, E., 2015. Vulnerability and resilience of transport systems - A discussion of recent research. Transportation Research Part A 81, 16–34.

Messner, F., Penning-Rowsell, E., Green, C., Meyer, V., Tunstall, S., van der Veen, A., 2007. Evaluating flood damages: guidance and recommendations on principles and methods. FLOODsite Consortium Wallingfor, 179pp.

Munich Re, 2014. Natural Catastrophes 2013. Topics Geo - Annual Review .

Narayanan, A., Willis, H.H., Fischbach, J.R., Warren, D., Molina-perez, E., Stelzner, C., Loa, K., Kendrick, L., Sorensen, P., Latourrette, T., 2016. Characterizing National Exposures to Infrastructure from Natural Disasters Data and Methods Documentation. Technical Report. RAND Homeland Security and Defense Center. URL: https://www.rand.org/pubs/research{_}reports/RR1453z1.html.

Pant, R., Thacker, S., Hall, J.W., Alderson, D., Barr, S., 2017. Critical infrastructure impact assessment due to flood exposure. Journal of Flood Risk Management 11, 22–33. doi:10.1111/jfr3.12288.

Pregnolato, M., Ford, A., Wilkinson, S.M., Dawson, R.J., 2017. The impact of flooding on road transport: A depth-disruption function. Transportation Research Part D 55, 67–81. doi:10.1016/j.trd.2017.06.020.

Qiang, Y., 2019. Flood exposure of critical infrastructures in the United States. International Journal of Disaster Risk Reduction 39, 101240. URL: https://linkinghub.elsevier.com/retrieve/pii/S2212420918314754, doi:10.1016/j.ijdrr.2019.101240.

Ramirez, J.A., Lichter, M., Coulthard, T.J., Skinner, C., 2016. Hyper-resolution mapping of regional storm surge and tide flooding: comparison of static and dynamic models. Natural Hazards 82, 571–590. doi:10.1007/s11069-016-2198-z.

Röthlisberger, V., Zischg, A.P., Keiler, M., 2017. Identifying spatial clusters of flood exposure to support decision making in risk management. Science of the Total Environment 598, 593–603.

Scott, D.M., Novak, D.C., Autumn-Hall, L., Guo, F., 2006. Network robustness index: A new method for identifying critical links and evaluating the performance of transportation networks. Journal of Transport Geography 14, 215–227.

Seneviratne, S., Nicholls, N., Easterling, D., Goodess, C., Kanae, S., Kossin, J., Luo, Y., Marengo, J., McInnes, K., Rahimi, M., Reichstein, M., Sorteberg, A., Vera, C., Zhang, X., 2012. Changes in climate extremes and their impacts on the natural physical environment. In: Managing the Risk of Extreme Events and Disasters to Advance Climate Change Adaptation.[Field, C.B., V. Barros, T.F. Stocker, D. Qin, D.J. Dokken, K.L. Ebi, M.D. Mastra. Technical Report. doi:10.2134/jeq2008.0015br, arXiv:1109.1006v1.

Tsiotas, D., 2017. Links between network topology and socioeconomic framework of railway transport: Evidence from Greece. Journal of Engineering Science and Technology Review 10, 175–187. doi:10.25103/jestr.103.23.

UNISDR, 2016. Report of the open-ended intergovernmental expert working group on indicators and terminology relating to disaster risk reduction. Technical Report. United Nations Office for Disaster Risk Reduction. URL: https://www.unisdr.org/we/inform/terminology.

Wang, S., Hong, L., Chen, X., Zhang, J., Yan, Y., 2011. Review of interdependent infrastructure systems vulnerability analysis. International Conference on Intelligent Control and Information Processing , 446–451.

Weaver, K.F., Morales, V.C., Dunn, S.L., Godde, K., Weaver, P.F., 2017. Pearson' s and Spearman's Correlation, in: An Introduction to Statistical Analysis in Research: With Applications in the Biological and Life Sciences. John Wiley & Sons, Inc. URL: https://onlinelibrary.wiley.com/doi/book/10.1002/9781119454205, doi:10.1002/9781119454205.

Zio, E., 2016. Challenges in the vulnerability and risk analysis of critical infrastructures. Reliability Engineering and System Safety 152.